

SOFTWARE NOTE

CuticleTrace: A toolkit for capturing cell outlines from leaf cuticle with implications for paleoecology and paleoclimatology

Benjamin A. Lloyd^{1,2}  | Richard S. Barclay³  | Regan E. Dunn^{4,5}  |
 Ellen D. Currano⁶  | Ayuni I. Mohamaad^{6,7} | Kymbre Skersies⁶ |
 Surangi W. Punyasena⁸ 

¹Department of Earth and Space Sciences, University of Washington, Johnson Hall Rm-070, Box 351310, 4000 15th Ave. NE, Seattle, Washington 98195-1310, USA

²Smithsonian Environmental Research Center, Smithsonian Institution, 647 Contees Wharf Rd., Edgewater, Maryland 21037-0028, USA

³Department of Paleobiology, National Museum of Natural History, Smithsonian Institution, 1000 Madison Dr. NW, Washington, D.C. 20560, USA

⁴La Brea Tar Pits and Museum, Natural History Museums of Los Angeles County, 5801 S. Wilshire Blvd., Los Angeles, California 90036, USA

⁵Department of Earth Sciences, University of Southern California, 3551 Trousdale Parkway, Los Angeles, California 90089, USA

⁶Department of Botany, University of Wyoming, 1000 E. University Ave., Laramie, Wyoming 82071, USA

⁷Department of Geological Sciences, University of Florida, 241 Williamson Hall, P.O. Box 112120, Gainesville, Florida 32611-2120, USA

⁸Department of Plant Biology, University of Illinois Urbana-Champaign, 139 Morrill Hall, 505 South Goodwin Ave., Urbana, Illinois 61801, USA

Correspondence

Benjamin A. Lloyd, Department of Earth and Space Sciences, University of Washington, Johnson Hall Rm-070, Box 351310, 4000 15th Ave. NE, Seattle, Washington 98195-1310, USA.

Email: blloyd96@uw.edu

Surangi W. Punyasena, Department of Plant Biology, University of Illinois Urbana-Champaign, 139 Morrill Hall, 505 South Goodwin Avenue, Urbana, Illinois 61801, USA.

Email: spunya1@illinois.edu

Abstract

Premise: Leaf epidermal cell morphology is closely tied to the evolutionary history of plants and their growth environments and is therefore of interest to many plant biologists. However, cell measurement can be time consuming and restrictive with current methods. CuticleTrace is a suite of Fiji and R-based functions that streamlines and automates the segmentation and measurement of epidermal pavement cells across a wide range of cell morphologies and image qualities.

Methods and Results: We evaluated CuticleTrace-generated measurements against those from alternate automated methods and expert and undergraduate hand tracings across a taxonomically diverse 50-image data set of variable image qualities. We observed ~93% statistical agreement between CuticleTrace and expert hand-traced measurements, outperforming alternate methods.

Conclusions: CuticleTrace is a broadly applicable, modular, and customizable tool that integrates data visualization and cell shape measurement with image segmentation, lowering the barrier to high-throughput studies of epidermal morphology by vastly decreasing the labor investment required to generate high-quality cell shape data sets.

KEYWORDS

cell shape, high-throughput phenotyping, image processing, image segmentation, leaf area index, leaf epidermis, paleobotany, paleoecology

The accurate, consistent, and efficient characterization of the leaf epidermis is key to advancing our understanding of the relationships of plants to their environments and their evolutionary history. The morphology and arrangement of

leaf epidermal cells vary significantly across different environmental conditions and taxonomic groups (Kürschner, 1997; Royer, 2001; Vófély et al., 2019). The shape of cell walls captures changes to canopy structure over geologic time

This is an open access article under the terms of the [Creative Commons Attribution-NonCommercial](https://creativecommons.org/licenses/by-nc/4.0/) License, which permits use, distribution and reproduction in any medium, provided the original work is properly cited and is not used for commercial purposes.

© 2024 The Authors. *Applications in Plant Sciences* published by Wiley Periodicals LLC on behalf of Botanical Society of America.

(Dunn et al., 2015; Bush et al., 2017; Milligan et al., 2021), and cell patterns and cell types can be used to enhance taxonomic resolution of paleofloras (e.g., Strömberg, 2011). When epidermal cells can be counted, the number of stomata relative to pavement cells has been used to constrain paleoenvironmental conditions such as atmospheric CO₂ concentration (McElwain and Chaloner, 1996; Royer, 2001). In crop science, phenomics links high-throughput phenotyping of leaf epidermal characters (e.g., cell size, shape, number) with genomics to breed plants with idealized physiological traits (Zhao et al., 2019).

Hand tracing has remained the most viable option for characterizing epidermal pavement cell morphology in most cases (e.g., Vófély et al., 2019; Brown and Jordan, 2023). Hand-traced data sets have been part of high-impact studies investigating cell shape, such as those using undulation index (UI) to determine the canopy position of fossil leaves (Kürschner, 1997), to estimate growing season characteristics from the cells of birch trees (Wagner-Cremer et al., 2010), and to determine canopy position of leaves by correlating UI with the $\delta^{13}\text{C}$ gradient present at increasing ground height (Bush et al., 2017; Graham et al., 2019). Cell wall undulation and aspect ratios have also been used to investigate hypotheses about pavement cell form and function within a phylogenetic context (Vófély et al., 2019) and to untangle the interactions between climate and the biota living in forests in a deep-time context (Dunn et al., 2015). These studies demonstrate

the relatively untapped potential of plant cell shape data sets, which can reveal changes to climate, ecosystems, and their influence on patterns in evolutionary biology that cannot be obtained with other methodologies.

Efforts to automate leaf epidermal measurement have met differing levels of success. Stomata can be efficiently identified from microscope images (e.g., Fetter et al., 2019; Li et al., 2022), but the accurate characterization of epidermal pavement cell morphologies remains limited to specific taxa or imaging techniques (Möller et al., 2017; Li et al., 2022). Hand tracing is a slow and tedious process, with cell-outline quality highly dependent upon both the tools used for tracing (e.g., mouse, stylus, tablet, desktop computer) and the experience level and conscientiousness of the tracer (e.g., Wagner-Cremer et al., 2010). The high labor requirement of hand tracing—and the non-standardized measurements that result—imposes a barrier to the use of epidermal cell shape in multiple disciplines.

We developed the CuticleTrace toolkit to streamline and automate the tracing and measurement of epidermal pavement cells. Our easily fine-tuned, open-source workflow uses the freeware software Fiji (Schindelin et al., 2012) and R Statistical Software (R Core Team, 2022). Our methodology can be applied across a wide variety of taxa, image qualities, and image preparations to generate large cell shape data sets from images of leaf cuticle or epidermis. The CuticleTrace process is fast, consistent, reproduces expert-level measurements, and produces much larger data sets than when drawn by hand.

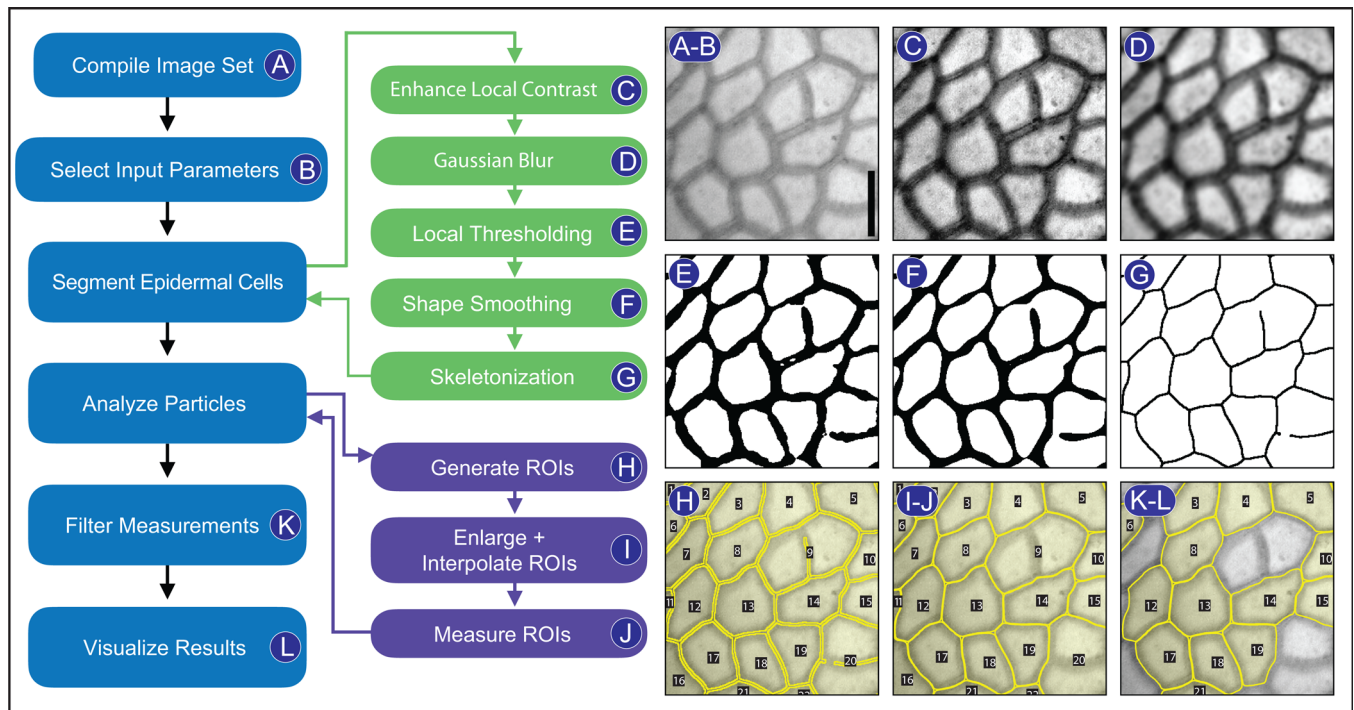


FIGURE 1 The processing workflow for the CuticleTrace toolkit (left) illustrated on an image of *Castanea pumila* L. (Fagaceae, FLMNH00115). Scale bar = 10 μm . Processing starts by (A) compiling an image set and (B) selecting input parameters. This is followed by epidermal cell segmentation, consisting of (C) local contrast enhancement, (D) Gaussian blur, (E) local thresholding, (F) shape smoothing, and (G) skeletonization. Particles are analyzed in Fiji, by (H) generating regions of interest (ROIs), (I) enlarging and interpolating ROIs, and (J) measuring ROIs. ROI measurements are (K) filtered with median statistics and (L) visualized overlaying unprocessed images.

METHODS AND RESULTS

CuticleTrace description

The CuticleTrace workflow consists of four steps. First, users determine appropriate batch-processing inputs with the “Single Image Processor” Fiji macro (Figure 1B). Second, users batch-process images and measure cells with the “Batch Generate ROIs” and “Batch Measure (Different Scales)” Fiji macros, which generate (1) thresholded and skeletonized binary images (Figures 1F, G), (2) sets of files

recording individual cell shapes known as “regions of interest” (ROIs; Figure 1I), and (3) shape parameter measurements associated with each ROI (Figure 1J). Third, the resulting cell measurements are filtered with median statistics by the “CuticleTrace Data Filtration” R Notebook (Figure 1K). Last, users can visualize the effects of data filtration with the “Batch Overlay” Fiji macro (Figure 1L).

An illustrated manual for the installation and use of Fiji and R tools is available in the CuticleTrace User Manual (available in the GitHub repository: <https://github.com/benjllloyd/CuticleTrace>; see Data Availability Statement). A video tutorial

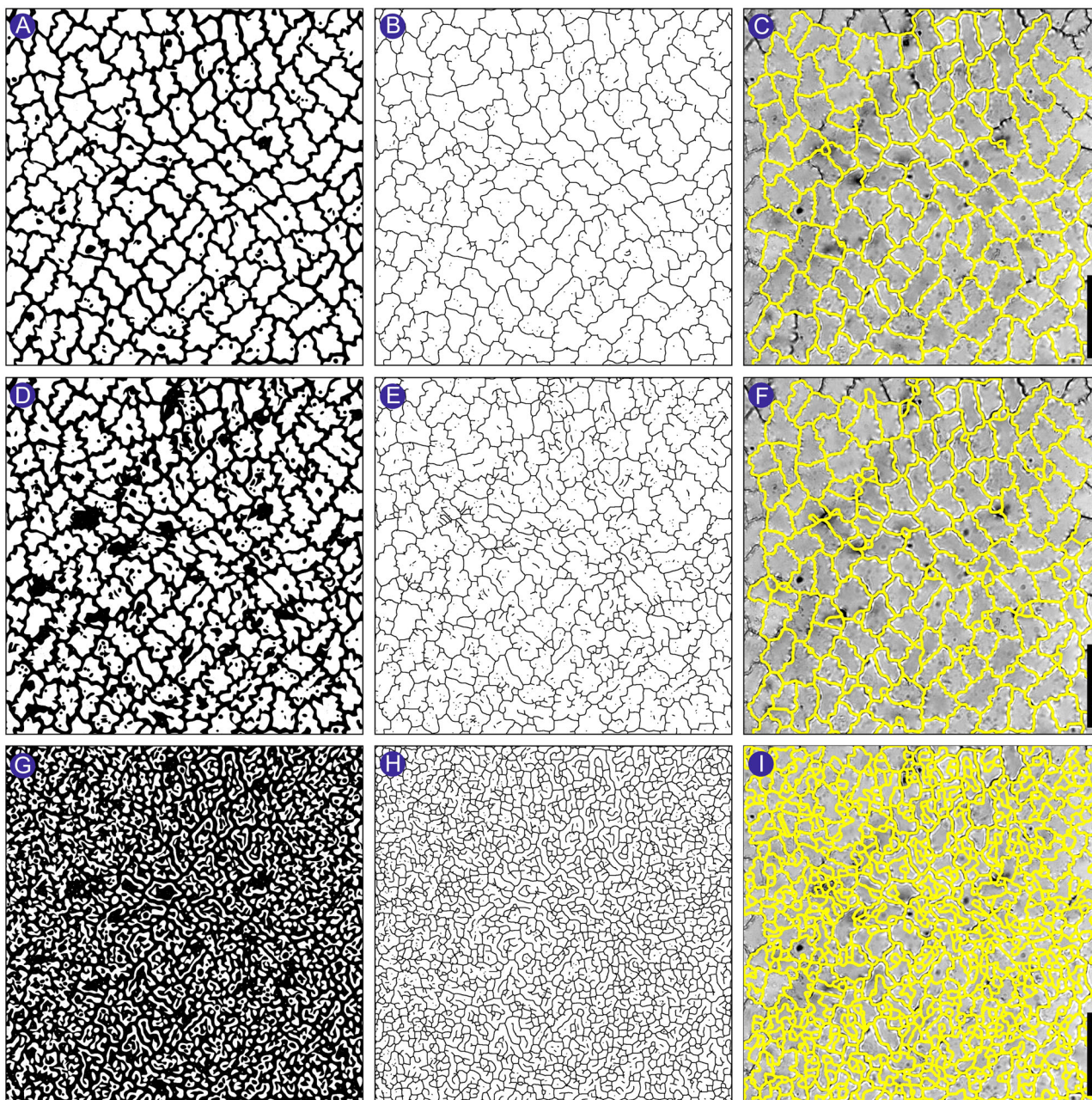


FIGURE 2 The effect of thresholding (A, D, G) on skeletonization (B, E, H) and unfiltered ROI sets (C, F, I), demonstrated on *Talisia princeps* Oliv. (Sapindaceae, FLMNH00443). The image is thresholded by (A–C) Sauvola local thresholding (ideal), (D–F) Bernsen local thresholding (satisfactory), and (G–I) NiBlack local thresholding (ineffective). Scale bars = 50 μm .

is available online (<https://youtu.be/XLhWd-tpU70>), and all software is documented on the CuticleTrace GitHub repository.

Determination of batch processing inputs

Both the “Single Image Processor” and “Batch Generate ROIs” macros apply seven user inputs to images. “Single Image Processor” works with an open image, while “Batch Generate ROIs” processes all images in an image set. Each user input sets the parameters for different image processing operations. Before batch-processing, users must first determine the appropriate input parameters on a small subset of images using the “Single Image Processor” macro. The selection of appropriate input parameters is extremely important to ensure accurate results (Figure 2). Detailed instructions for user input selection are provided in section 4.1 of the CuticleTrace User Manual (see Data Availability Statement), which includes examples of images with optimal and suboptimal values for all inputs.

For both macros, users select: (1) whether cell walls are dark on a light background or light on a dark background, (2) the standard deviation of Gaussian blur (Figure 1D), (3) the automated local thresholding algorithm (Figures 1E, 2), (4) the initial local thresholding radius (Figure 1E), (5) the range of sizes (in pixels squared) of all cells expected in the image set (Figure 1E), (6) the percentage of Fourier descriptors to retain during shape smoothing (Figure 1F), and (8) the scale (in pixels/unit) of all images in the image set (Figure 1J).

Image processing and measurement

The “Batch Generate ROIs” macro outputs thresholded and skeletonized binary images, and unfiltered (enhanced and interpolated) ROI sets of all images in a directory (Figure 1C–I). Users may also elect to output measurements of ROI shape parameters if all images have the same scale, or use “Batch Measure (Different Scales)” to measure ROIs of images with differing scales (Figure 1J, Table 1). These unfiltered ROI sets and measurement files may then be brought directly into the “CuticleTrace Data Filtration” R Notebook for statistical filtration.

Data filtration

The ROIs produced by the CuticleTrace Fiji analysis pipeline will inevitably include partial cells, multiple cells, vein cells, or non-cuticle image artifacts (e.g., slide background, debris). The “CuticleTrace Data Filtration” R Notebook removes these erroneous data points by excluding ROIs with measurements outside one or two median absolute deviations (MADs) from each image’s median area, perimeter, circularity, aspect ratio, roundness, and solidity (Table 1). The R Notebook creates new ROI sets of the remaining ROIs after filtering (Figure 3).

TABLE 1 Descriptions or equations of all shape parameters measured by CuticleTrace.

Measurement parameter	Description or equation
Area	The area of an ROI.
Perimeter	The length of the outside boundary of an ROI.
Bounding rectangle	The x - y coordinates and dimensions of the smallest rectangle that encloses an ROI.
Fit ellipse	The dimensions and orientation of an ellipse fit to an ROI.
Feret's diameter	The longest distance between any two points on the ROI boundary.
Minimum Feret's diameter	The minimum caliper diameter of an ROI.
Circularity	$4\pi * \frac{[Area]}{[Perimeter]^2}$
Aspect ratio	$\frac{[Major Axis of Fit Ellipse]}{[Minor Axis of Fit Ellipse]}$
Roundness	$4 * \frac{[Area]}{\pi * [Major Axis of Fit Ellipse]^2}$
Solidity	$\frac{[Area]}{[Area of Convex Hull]}$
Undulation index	$\frac{[Perimeter]}{2\pi * \sqrt{[Area]}/\pi}$

Note: ROI = region of interest.

We use the median as our reference point because unfiltered measurements are non-normally distributed (Figure 4). Using the median, rather than the mean, allowed us to work efficiently with the skewed distribution of ROIs and identify erroneous outliers. Distribution around the median captured the central tendency of cell size or shape. The limitation of using deviation from the median, however, is that it requires a large number of ROIs to be effective. If there are only a limited number of ROIs or few erroneous outliers, this threshold will discard a large percentage of accurate measurements. For this reason, users should visualize outlines, before and after filtering, in order to determine whether the choice of threshold meets the specific needs of their images.

Data visualization

The “Batch Overlay” Fiji macro allows users to visualize CuticleTrace outputs by creating images overlain with outlines of each ROI in an ROI set, formatted to the user’s preference. “Batch Overlay” may be used to overlay any batch of ROI sets on any batch of images. In our evaluation, we used “Batch Overlay” to visually check the accuracy of ROIs resulting from different input parameters (Figure 2) and to compare unfiltered ROI sets with the filtered versions from the “CuticleTrace Data Filtration” R Notebook (Figures 3 and 4).

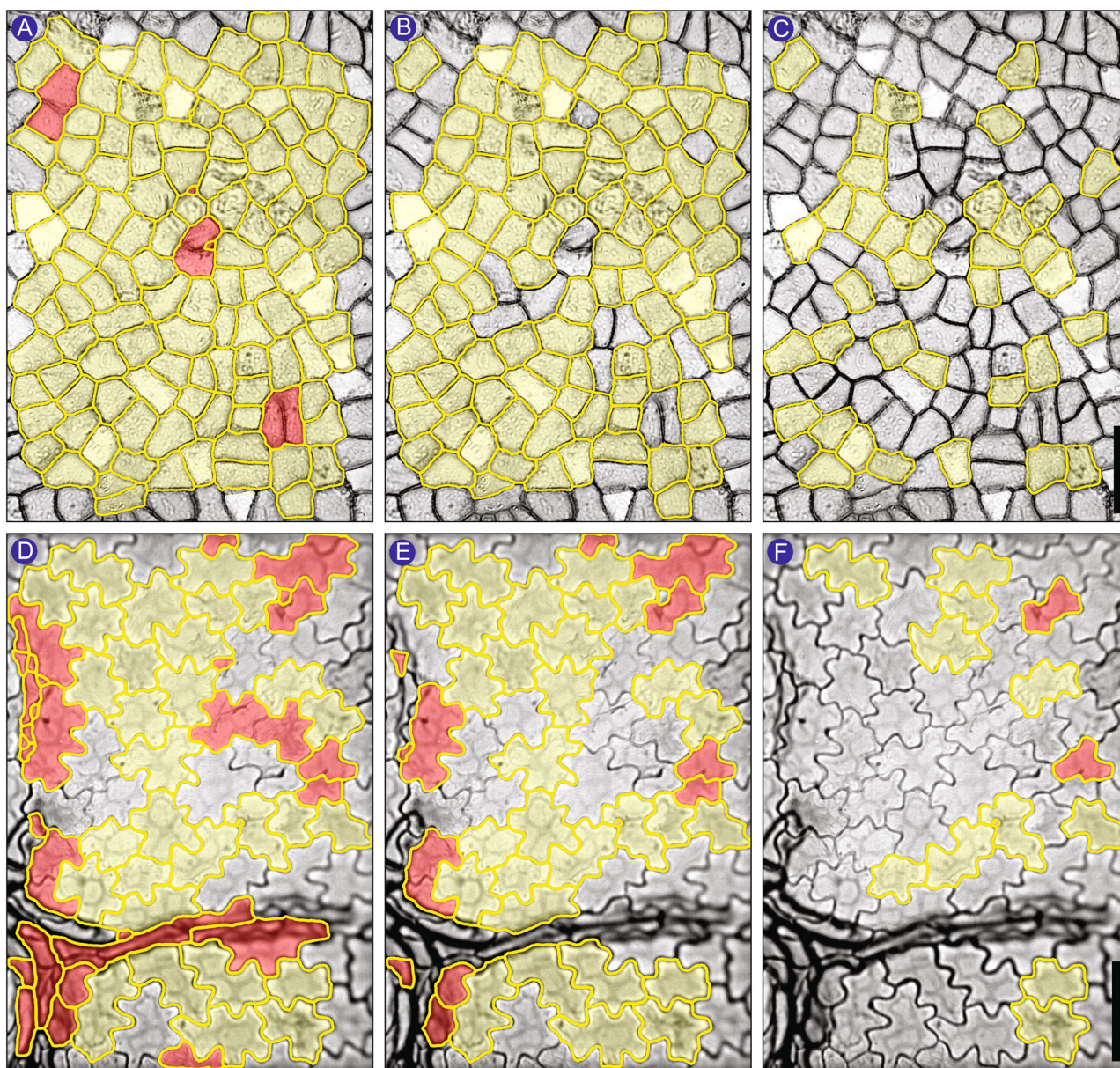


FIGURE 3 Removal of unwanted ROIs by filtering using median statistics. (A–C) *Ocotea tarapotana* (Meisn.) Mez (Lauraceae, FLMNH00185); (D–F) *Acer skutchii* Rehder (Aceraceae, FLMNH00714). ROI sets that are (A, D) unfiltered, (B, E) $\pm 2\text{MAD}$ -filtered, and (C, F) $\pm 1\text{MAD}$ -filtered. Yellow outlines represent ROIs retained at each filtering level. Yellow-shaded ROIs accurately characterize epidermal pavement cells and are thus wanted in the final data set. Red-shaded ROIs do not accurately characterize pavement cells and are thus not wanted in the final data set. Scale bars = 50 μm .

CuticleTrace evaluation

We evaluated CuticleTrace across a range of image resolutions, magnifications, and qualities, using an image set of 50 vouchered herbarium specimens from the Cuticle Database (<https://cuticledb.eesi.psu.edu>; Barclay et al., 2007). Images were chosen to maximize taxonomic breadth (48 species, 37 genera, 20 families) and span the range of cell shapes and sizes (Appendix S1). We generated CuticleTrace measurements following the protocol outlined in the CuticleTrace User Manual (see Data Availability Statement), with user inputs specified in Table 2.

We compared CuticleTrace measurements (at the $\pm 1\text{MAD}$ and $\pm 2\text{MAD}$ filtering levels) to hand-traced outlines. An expert (R.E.D.) and University of Wyoming undergraduates (A.I.M., K.S.) each outlined 10 cells per image following Dunn et al. (2015). Cells for each tracer were independently selected based on their position relative to an arbitrarily positioned sampling grid. We also compared CuticleTrace to measurements generated by alternative automated segmentation methods (LeafNet [Li et al., 2022] and PaCeQuant [Möller et al., 2017]). PaCeQuant did not successfully segment our light-microscopy images (unsurprising, as it was developed for confocal microscopy images) and was excluded from statistical comparisons of segmentation methods.

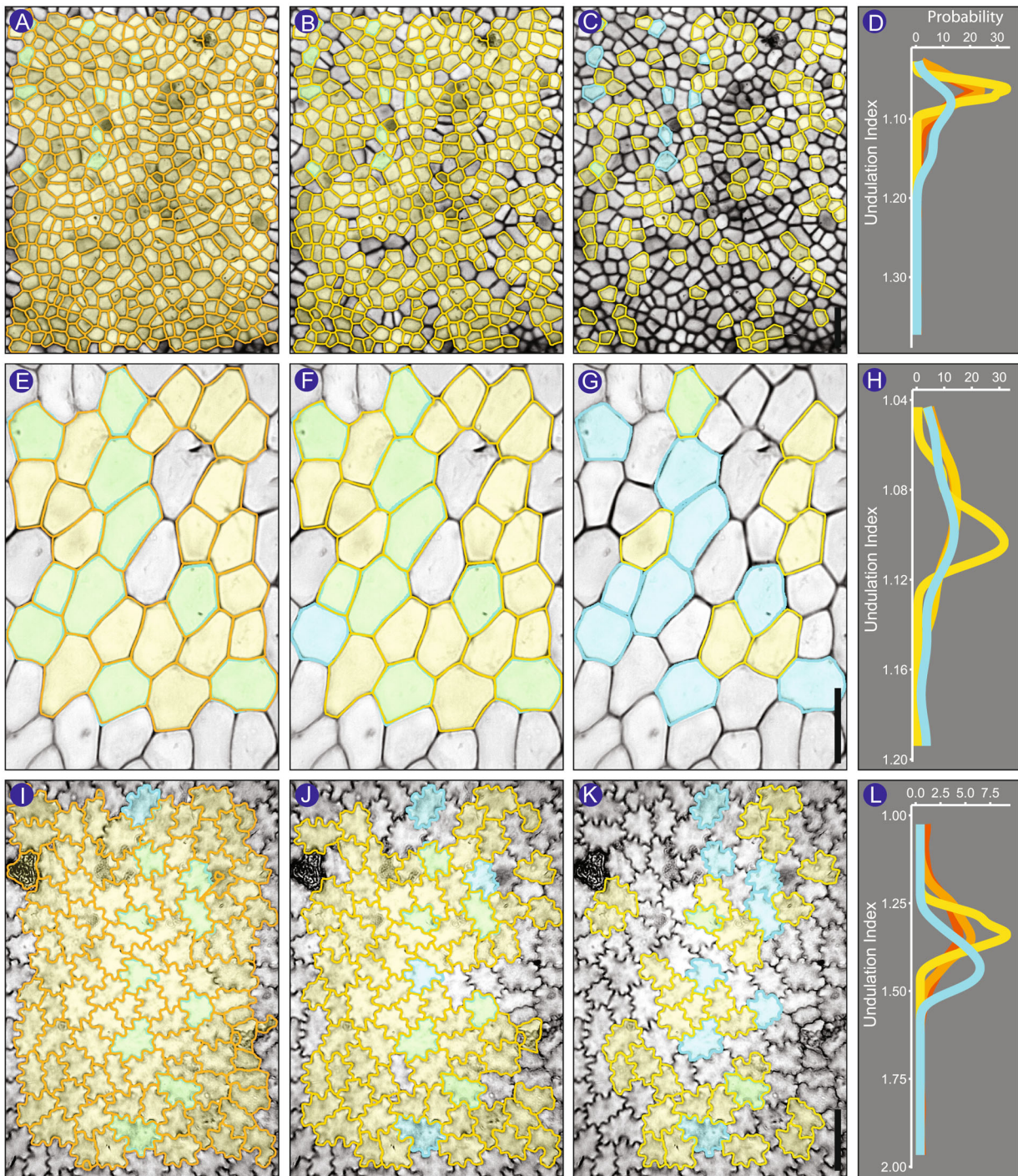


FIGURE 4 CuticleTrace-generated ROI sets (yellow) compared to expert hand-drawn ROI sets (cyan), with subsequent filtering using median statistics. Cells with overlapping CuticleTrace and expert-generated ROIs appear green. Columns show ROI sets that are (A, E, I) unfiltered, (B, F, J) ± 2 MAD, and (C, G, K) ± 1 MAD overlain on the source images of (A–C) *Nectandra oppositifolia* Nees & Mart. (Lauraceae, FLMNH00260), (E–G) *Guarea bijuga* C. DC. (Meliaceae, FLMNH00850), and (I–K) *Anaxagorea petiolata* R. E. Fr. (Annonaceae, FLMNH02589). (D, H, L) Probability density plots showing distributions of undulation index values across all four data sets for each image; hand-traced = cyan, unfiltered = dark orange, ± 2 MAD = light orange, ± 1 MAD = yellow. Scale bars = 50 μ m.

Finally, we completed a one-to-one comparison of CuticleTrace and expert measurements across all images. We selected the CuticleTrace outlines that directly corresponded to the subset of 10 expert hand-traced outlines. A total of 447 cells across all 50 images were shared between the two data sets.

Whole image comparison

The expert outlines served as our evaluation benchmark. We ran a one-way analysis of variance (ANOVA) with post-hoc nonparametric Games–Howell analysis for each shape

parameter for each image. We selected the Games–Howell test due to differing sample sizes between the four sets of measurements. We used CuticleTrace's “Batch Overlay” macro to visually compare CuticleTrace and expert tracings (Appendix S1).

Our analyses showed 100% statistical agreement between CuticleTrace measurements (at both $\pm 1\text{MAD}$ and $\pm 2\text{MAD}$ filtering levels) and expert measurements of area, perimeter, Feret's diameter, aspect ratio, and roundness (Figure 5). We observed variability in circularity, solidity, and UI measurements, which was expected due to their sensitivity to small tracing differences. CuticleTrace measurements consistently aligned more closely with expert measurements than expert measurements did with student and LeafNet measurements (Table 3).

TABLE 2 CuticleTrace batch-processing inputs for our 50-image test data set.

Input parameter	Value
Cell walls on background	Dark on light
Gaussian blur σ	2 pixels
Thresholding algorithm	Sauvola (Sauvola and Pietikäinen, 2000)
Initial thresholding radius	50 pixels
ROI size filter	500–50,000 pixels ²
Smoothing value	5% of Fourier descriptors

Cell-to-cell comparison

Our cell-to-cell comparison of CuticleTrace and expert measurements of individual cells (447 cells across all 50 images) showed broad agreement across all shape parameters (Figure 6). In only 11 of 400 image measurements (50 images, eight shape parameters) were values significantly different at the 2-sigma level—a 2.75% error rate. Seven of the 11 significant differences are concentrated in three images (identified in the Cuticle Database by their Florida Museum of Natural History specimen numbers)—FLMNH00178 (*Damburneya salicifolia* (Kunth) Trofimov & Rohwer), FLMNH00561 (*Gleditsia triacanthos* L.), and FLMNH05215 (*Peteniodendron durlandii* (Standl.) Baehni) (Figure 6). However, overall, differences between expert and CuticleTrace tracings were small, and CuticleTrace tracings were reasonable and consistent even when they differed from expert tracings.

Accuracy of CuticleTrace measurements

Across the wide range of cell shapes and image qualities encapsulated in our test data set (Appendix S1), CuticleTrace produces cell shape measurements that are statistically identical to expert measurements across all shape parameters in most instances, at both the $\pm 1\text{MAD}$ and $\pm 2\text{MAD}$ filtering level. The limited, often non-significant, differences between expert and CuticleTrace measurements may be attributed to two sources of variation. First, the set of cells outlined by CuticleTrace may differ from those traced by an expert in the same image.

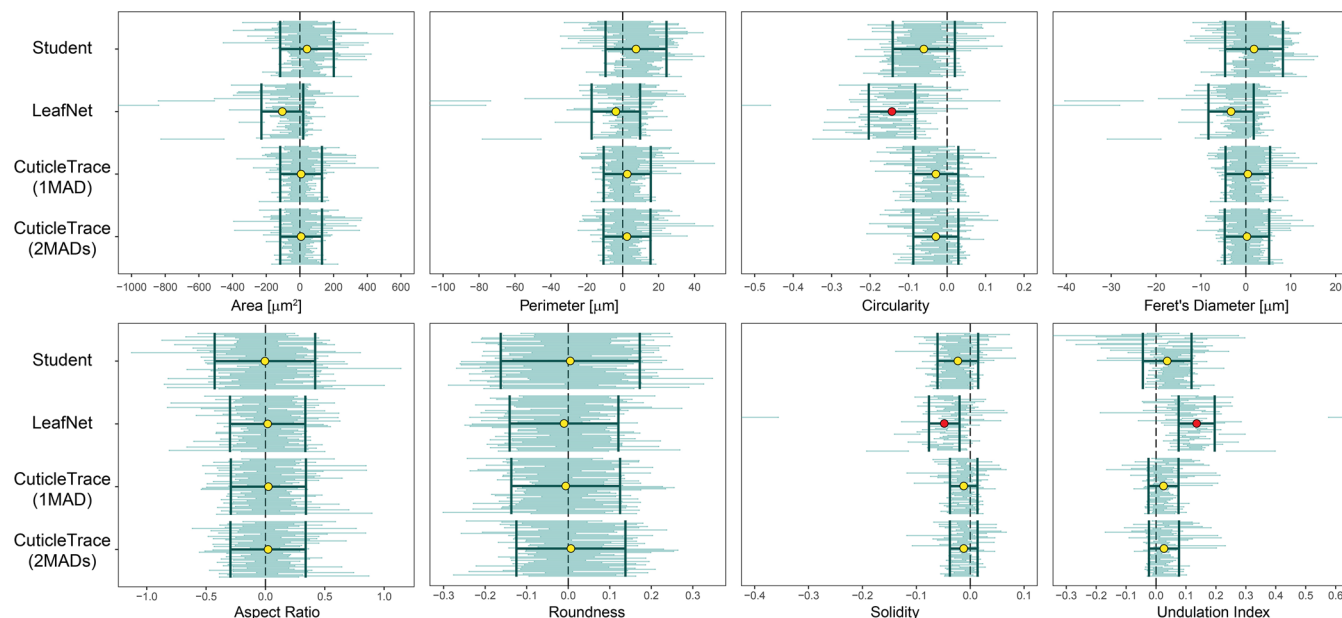


FIGURE 5 Post-hoc Games–Howell results for all 50 images, separated by shape parameter. Comparisons are all relative to the hand-drawn expert results (zero). Student data was also hand-drawn; LeafNet and CuticleTrace are automated methods. Each small horizontal bar represents the 95% confidence interval of the Games–Howell mean difference estimate applied to a single image in the comparative data set. The image position in the stack is maintained for each shape parameter. Darker bars with center circles are the mean $\pm 2\sigma$ for each of the comparative stacks of Games–Howell results. Yellow center circles are non-significant; red center circles are significantly different from the expert.

TABLE 3 Statistical evaluation of $\pm 1\text{MAD}$ and $\pm 2\text{MAD}$ CuticleTrace measurements, student measurements, and LeafNet measurements, in comparison to expert measurements.

Shape parameter	Average Games–Howell <i>P</i> value in comparison to expert					% of measurements statistically identical to expert (<i>P</i> values > 0.05)				
	CuticleTrace		Cell to cell	Student	LeafNet	CuticleTrace		Cell to cell	Student	LeafNet
	$\pm 1\text{MAD}$	$\pm 2\text{MAD}$				$\pm 1\text{MAD}$	$\pm 2\text{MAD}$			
Area	0.85	0.89	0.56	0.74	0.55	100	100	100	94	84
Perimeter	0.82	0.82	0.68	0.54	0.60	100	100	100	86	82
Feret's diameter	0.85	0.88	0.64	0.66	0.72	100	100	100	94	88
Circularity	0.52	0.53	0.44	0.31	0.06	78	82	94	58	12
Aspect ratio	0.79	0.82	0.88	0.75	0.81	100	100	100	100	100
Roundness	0.78	0.82	0.88	0.81	0.78	100	100	100	100	100
Solidity	0.44	0.47	0.42	0.34	0.18	76	78	90	72	30
Undulation index	0.52	0.53	0.44	0.25	0.06	82	88	94	52	12
Mean	0.70	0.72	0.62	0.55	0.47	92.0	93.5	97.3	82.0	63.5

However, CuticleTrace generates a much larger cell measurement data set than is possible by hand. Therefore, provided the cells selected by CuticleTrace are representative of the whole image, the differences between the two methods were more likely a result of bias in the hand-drawn cells, as the grid-selection method of hand tracing results in smaller sample sizes and tends to favor larger cells.

Second, CuticleTrace may emphasize different aspects of cell morphology than an expert. Crenulated cells with obvious three-dimensional morphology showed the greatest number of disagreements (Figure 6A, D). In these images, the expert chose to outline the cell wall at an alternate focal level than the CuticleTrace macros. The choice of focal level is somewhat subjective, however, and CuticleTrace's interpretation of the cell outline was largely reasonable and consistent. Our cell-to-cell comparison of 447 individual cells across 50 images showed that expert and CuticleTrace measurements are highly correlated (Figure 6). For most images, CuticleTrace and expert measurements were effectively interchangeable.

The ease of data visualization built into CuticleTrace with the “Batch Overlay” and “Single Image Processor” macros is an important feature for ensuring accurate cell tracing and ROI filtering. Our design makes the qualitative assessment of outputs easy, so that users can visually check all CuticleTrace outputs—thresholded images, skeletonized images, and filtered and unfiltered ROI sets—and modify input parameters as necessary. Additionally, CuticleTrace users may modify the “CuticleTrace Data Filtration” R Notebook to suit their needs, and ROI sets may always be manually revised in Fiji.

Slide preparation, image quality, and CuticleTrace input parameters were the most important factors in ensuring accuracy in automated measurements. While we intentionally included a wide range of image qualities in our data set (Appendix S1), we did not attempt to analyze Cuticle Database images that were of very poor quality. CuticleTrace's flexibility allows it to be fine-tuned for a wide variety of image

preparations and resolutions, but that same flexibility may lead to ineffective or inaccurate image characterization if users neglect to carefully select input parameters (Figure 2). It is imperative that users closely follow the instructions provided in the CuticleTrace User Manual (see Data Availability Statement).

Comparison to other automated methods

CuticleTrace is a unique addition to the suite of available methodologies for automatically segmenting and characterizing leaf epidermal morphology. Other approaches—PaCeQuant (Möller et al., 2017) and LeafNet (Li et al., 2022)—also automate epidermal pavement cell segmentation, with some limitations. Many other methods focus on stomata detection and characterization (e.g., Fetter et al., 2019; Li et al., 2022), while additional methods have been developed to trace cells in other plant tissues (Wolny et al., 2020) and cell outlines from a broad taxonomic training set of microscopic images (Stringer et al., 2021).

Of these methods, CuticleTrace is the first to effectively trace and measure epidermal pavement cells across a wide variety of taxa, cell morphologies, and image qualities. The customizability of the “Batch Generate ROIs” and “Single Image Processor” Fiji macros allows users to tune CuticleTrace's settings to work well for their images. Unlike machine learning approaches to cell segmentation, CuticleTrace does not require training images and can work with a broad range of morphologies using existing Fiji tools. It can therefore be more easily applied to studies involving diverse samples, detrital cuticle, or extinct taxa.

CuticleTrace's current inability to detect and mask stomata limits its use on stomata-rich abaxial cuticle and with other non-pavement epidermal cells, e.g., trichome bases and subsidiary cells. The toolkit is able to segment and outline these cell types if the cell walls are in focus but will not distinguish them from pavement cells. Users could

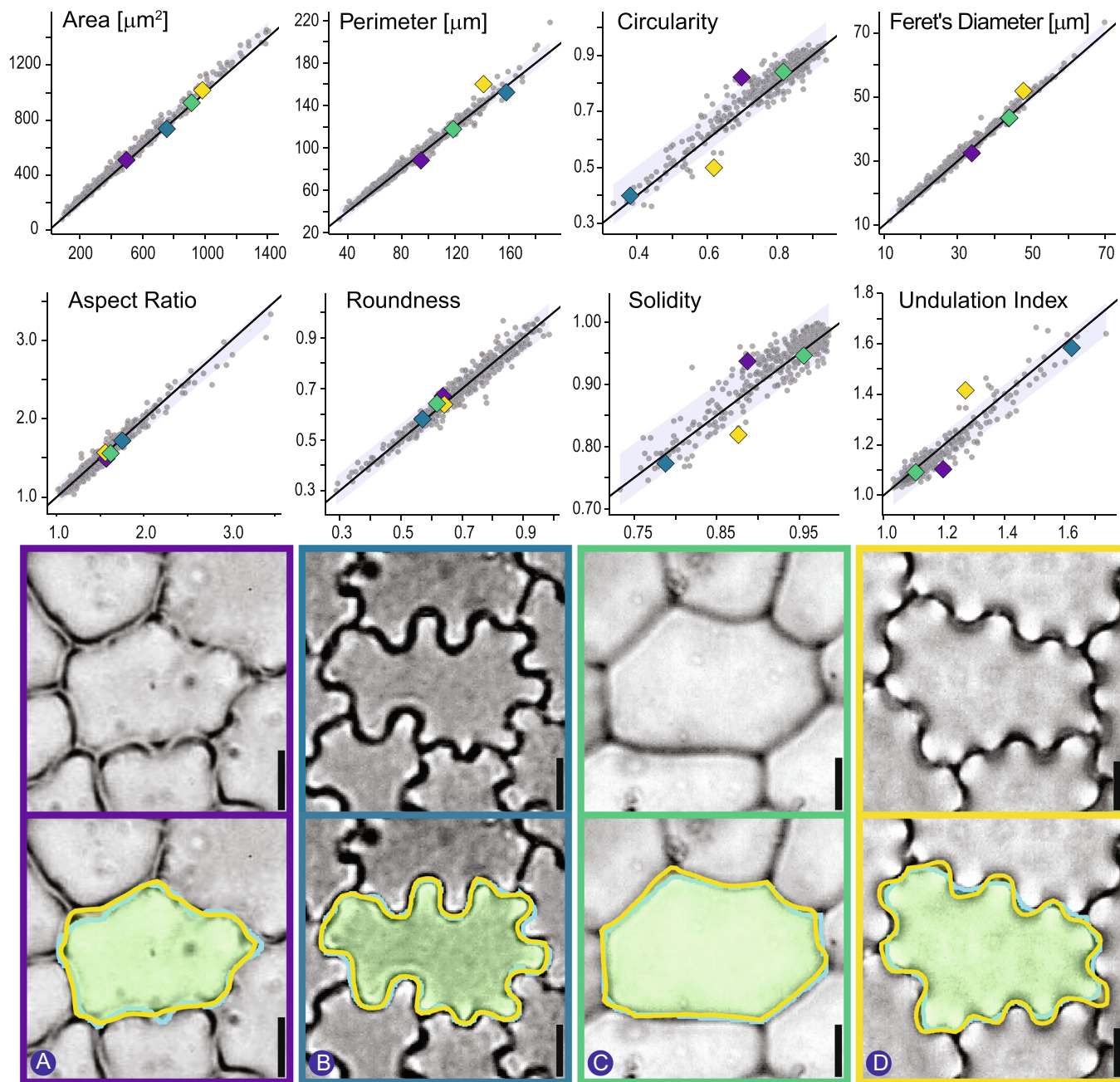


FIGURE 6 Cell-to-cell comparison of expert and CuticleTrace measurements. Upper panel: Correlation between expert (x -axis) and CuticleTrace (y -axis) measurements across 447 cells and all relevant shape parameters, distributed between 50 images. Black lines have a slope of 1, indicating 100% correlation. Shaded areas show 95% prediction intervals. Colored symbols correlate to the four images presented in the lower panel, which provides a visual comparison of the difference between cell outlines hand drawn by an expert (cyan line) vs. the CuticleTrace automated procedure (yellow line). Lower panel: (A) *Gleditsia triacanthos* L. (Fabaceae, FLMNH00081); (B) *Toxicodendron striatum* (Ruiz & Pav.) Kuntze (Anacardiaceae, FLMNH00510); (C) *Oreopanax capitatus* (Jacq.) Decne. & Planch. (Araliaceae, FLMNH00767); (D) *Peteniodendron durlandii* (Stand.) Lundell (Sapotaceae, FLMNH05215). Scale bars = 10 μm .

potentially identify non-pavement cells by their distinct shape parameters and isolate their respective ROIs by filtering by those parameters. CuticleTrace's ability to visualize filtered ROIs provides an easy check of any modifications to the filtering steps within the R Notebook. Alternatively, specific ROIs can be removed manually within Fiji. The toolkit's modular structure also allows for

the integration of machine learning-based methods for stomatal recognition and masking (Fetter et al., 2019; Aono et al., 2021; Li et al., 2022; Sai et al., 2023). With its potential for integration with other methods and software, CuticleTrace represents a robust foundation for image binarization, ROI generation, and morphological analysis that may find multiple applications in plant science.

CONCLUSIONS

The modularity and adaptability of the CuticleTrace toolkit hold great potential for its use in applications beyond those described here. CuticleTrace allows for the interchange of different parts of its analysis pipeline for alternate applications, and we intend for the toolkit to remain in active development. The local thresholding methods employed by CuticleTrace are effective for segmenting epidermal pavement cells in light microscopy images, but alternative segmentation methods (Möller et al., 2017; Wolny et al., 2020; Stringer et al., 2021; Li et al., 2022; Kirillov et al., 2023) can be swapped into the CuticleTrace pipeline as needed for other applications. Additional refinements and improvements to image thresholding and skeletonization can also be incorporated as these functions are added by the ImageJ community. Alternative approaches to the morphological analysis of epidermal cells (e.g., Möller et al., 2017; Nowak et al., 2021; Brown and Jordan, 2023) can also utilize CuticleTrace-generated ROIs to measure shape parameters beyond those included within CuticleTrace.

The leaf epidermis contains a wealth of information about the evolutionary history of plants and their growth environments, and CuticleTrace makes that information significantly more accessible. In both living and fossil plants, epidermal pavement morphology can be used to gain insight into plant physiology, ecology, and evolution, and fossil evidence of epidermal cells is integral to some paleoenvironmental studies. The largest barrier to big-data approaches to these questions is the non-trivial task of accurately segmenting epidermal cell images. CuticleTrace represents a significant advance, greatly lowering the barrier to high-throughput studies of epidermal morphology by increasing the consistency of epidermal cell measurements and by vastly decreasing the labor investment required to generate cell shape data sets.

AUTHOR CONTRIBUTIONS

B.A.L., R.S.B., R.E.D., and S.W.P. conceived the study. B.A.L. conducted the data analysis and created the Fiji image processing macros and R filtering code. R.E.D., K.S., and A.I.M. provided manual cell outlines. R.E.D. and E.D.C. recruited and supervised the University of Wyoming students. B.A.L. and S.W.P. wrote the manuscript with help from R.S.B. and R.E.D. R.S.B. and S.W.P. supervised and directed the research. All authors approved the final version of the manuscript.

ACKNOWLEDGMENTS

The authors thank Matilda Brown and an anonymous reviewer for constructive feedback that helped us improve the manuscript. R.S.B. acknowledges financial support from the National Science Foundation (NSF; grant EAR:1805228). S.W.P. acknowledges support from a 2022 University of Illinois National Center for Supercomputing Applications (NCSA) Faculty Fellowship. E.D.C., R.E.D., K.S., and A.I.M. acknowledge support from NSF grant EAR:145031. B.A.L. acknowledges financial support from Caroline Strömberg

(University of Washington) and thanks her, Alex Lowe (University of Washington), and Elena Stiles (University of Washington) for constructive discussion.

DATA AVAILABILITY STATEMENT

All generated and analyzed data from this study are included in the published article and its Supporting Information (Appendix S1). The CuticleTrace User Manual, code for the Fiji macros, and the R Notebook for filtering cells are available in the GitHub repository (<https://github.com/benjllloyd/CuticleTrace>). A video tutorial is available at <https://youtu.be/XLhWd-tpU70>.

ORCID

Benjamin A. Lloyd  <http://orcid.org/0000-0001-6749-2386>
 Richard S. Barclay  <http://orcid.org/0000-0003-4979-6970>
 Regan E. Dunn  <http://orcid.org/0000-0002-6042-0619>
 Ellen D. Currano  <http://orcid.org/0000-0002-5242-8573>
 Surangi W. Punyasena  <http://orcid.org/0000-0003-2110-5840>

REFERENCES

- Aono, A. H., J. S. Nagai, G. da S. M. Dickel, R. C. Marinho, P. E. A. M. de Oliveira, J. P. Papa, and F. A. Faria. 2021. A stomata classification and detection system in microscope images of maize cultivars. *PLoS ONE* 16: e0258679.
- Barclay, R., J. McElwain, D. Dilcher, and B. Sageman. 2007. The Cuticle Database: Developing an interactive tool for taxonomic and paleoenvironmental study of the fossil cuticle record. *Courier Forschungsinstitut Senckenberg* 258: 39–55.
- Brown, M. J. M., and G. J. Jordan. 2023. No cell is an island: Characterising the leaf epidermis using epidermalmorph, a new R package. *New Phytologist* 237: 354–366.
- Bush, R. T., J. Wallace, E. D. Currano, B. F. Jacobs, F. A. McInerney, R. E. Dunn, and N. J. Tabor. 2017. Cell anatomy and leaf $\delta^{13}\text{C}$ as proxies for shading and canopy structure in a Miocene forest from Ethiopia. *Palaeogeography, Palaeoclimatology, Palaeoecology* 485: 593–604.
- Dunn, R. E., C. A. E. Strömberg, R. H. Madden, M. J. Kohn, and A. A. Carlini. 2015. Linked canopy, climate, and faunal change in the Cenozoic of Patagonia. *Science* 347: 258–261.
- Fetter, K. C., S. Eberhardt, R. S. Barclay, S. Wing, and S. R. Keller. 2019. StomataCounter: A neural network for automatic stomata identification and counting. *New Phytologist* 223: 1671–1681.
- Graham, H. V., F. Herrera, C. Jaramillo, S. L. Wing, and K. H. Freeman. 2019. Canopy structure in Late Cretaceous and Paleocene forests as reconstructed from carbon isotope analyses of fossil leaves. *Geology* 47(10): 977–981.
- Kirillov, A., E. Mintun, N. Ravi, H. Mao, C. Rolland, L. Gustafson, T. Xiao, et al. 2023. Segment Anything. arXiv [Preprint]. Available at: <https://arxiv.org/abs/2304.02643> [posted 5 April 2023; accessed 2 January 2024].
- Kürschner, W. M. 1997. The anatomical diversity of recent and fossil leaves of the durmast oak (*Quercus petraea* Lieblein/*Q. pseudocastanea* Goepfert) — implications for their use as biosensors of palaeoatmospheric CO_2 levels. *Review of Palaeobotany and Palynology* 96: 1–30.
- Li, S., L. Li, W. Fan, S. Ma, C. Zhang, J. C. Kim, K. Wang, et al. 2022. LeafNet: A tool for segmenting and quantifying stomata and pavement cells. *The Plant Cell* 34: 1171–1188.
- McElwain, J. C., and W. G. Chaloner. 1996. The fossil cuticle as a skeletal record of environmental change. *PALAIOS* 11: 376–388.
- Milligan, J. N., A. G. Flynn, J. D. Wagner, L. L. R. Kouwenberg, R. S. Barclay, B. W. Byars, R. E. Dunn, et al. 2021. Quantifying the effect of shade on cuticle morphology and carbon isotopes of sycamores: Present and past. *American Journal of Botany* 108: 2435–2451.

- Möller, B., Y. Poeschl, R. Plötner, and K. Bürstenbinder. 2017. PaCeQuant: A tool for high-throughput quantification of pavement cell shape characteristics. *Plant Physiology* 175: 998–1017.
- Nowak, J., R. C. Eng, T. Matz, M. Waack, S. Persson, A. Sampathkumar, and Z. Nikoloski. 2021. A network-based framework for shape analysis enables accurate characterization of leaf epidermal cells. *Nature Communications* 12(1): 458.
- R Core Team. 2022. R: A Language and Environment for Statistical Computing. R Foundation for Statistical Computing, Vienna, Austria. Website: <http://www.R-project.org/> [accessed 2 January 2024].
- Royer, D. L. 2001. Stomatal density and stomatal index as indicators of paleoatmospheric CO₂ concentration. *Review of Palaeobotany and Palynology* 114: 1–28.
- Sai, N., J. P. Bockman, H. Chen, N. Watson-Haigh, B. Xu, X. Feng, A. Piechatzek, et al. 2023. StomaAI: An efficient and user-friendly tool for measurement of stomatal pores and density using deep computer vision. *New Phytologist* 238: 904–915.
- Sauvola, J., and M. Pietikäinen. 2000. Adaptive document image binarization. *Pattern Recognition* 33(2): 225–236. [https://doi.org/10.1016/s0031-3203\(99\)00055-2](https://doi.org/10.1016/s0031-3203(99)00055-2)
- Schindelin, J., I. Arganda-Carreras, E. Frise, V. Kaynig, M. Longair, T. Pietzsch, S. Preibisch, et al. 2012. Fiji: An open-source platform for biological-image analysis. *Nature Methods* 9: 676–682.
- Stringer, C., T. Wang, M. Michaelos, and M. Pachitariu. 2021. Cellpose: A generalist algorithm for cellular segmentation. *Nature Methods* 18: 100–106.
- Strömberg, C. A. E. 2011. Evolution of grasses and grassland ecosystems. *Annual Review of Earth and Planetary Sciences* 39: 517–544.
- Vófély, R. V., J. Gallagher, G. D. Pisano, M. Bartlett, and S. A. Braybrook. 2019. Of puzzles and pavements: A quantitative exploration of leaf epidermal cell shape. *New Phytologist* 221: 540–552.
- Wagner-Cremer, F., W. Finsinger, and A. Moberg. 2010. Tracing growing degree-day changes in the cuticle morphology of *Betula nana* leaves: A new micro-phenological palaeo-proxy. *Journal of Quaternary Science* 25(6): 1008–1017.
- Wolny, A., L. Cerrone, A. Vijayan, R. Tofanelli, A. V. Barro, M. Louveaux, C. Wenzl, et al. 2020. Accurate and versatile 3D segmentation of plant tissues at cellular resolution. *eLife* 9: e57613.
- Zhao, C., Y. Zhang, J. Du, X. Guo, W. Wen, S. Gu, J. Wang, and J. Fan. 2019. Crop phenomics: Current status and perspectives. *Frontiers in Plant Science* 10: 714. <https://doi.org/10.3389/fpls.2019.00714>

SUPPORTING INFORMATION

Additional supporting information can be found online in the Supporting Information section at the end of this article.

Appendix S1. Images of ROI outputs from CuticleTrace (Unfiltered, $\pm 1\text{MAD}$, $\pm 2\text{MAD}$) and expert hand tracing on all 50 images in our test data set.

How to cite this article: Lloyd, B. A., R. S. Barclay, R. E. Dunn, E. D. Currano, A. I. Mohamaad, K. Skersies, and S. W. Punyasena. 2024. CuticleTrace: A toolkit for capturing cell outlines from leaf cuticle with implications for paleoecology and paleoclimatology. *Applications in Plant Sciences* 12(1): e11566. <https://doi.org/10.1002/aps3.11566>